Journal of Materials Chemistry C

Accepted Manuscript

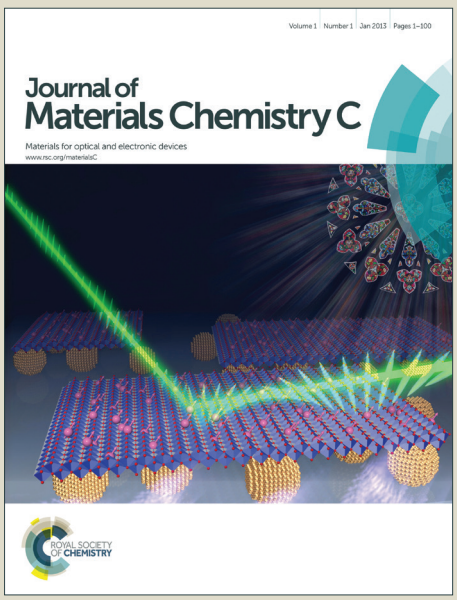

ROYAL SOCIETY OF CHEMISTRY

www.rsc.org/materialsC

A new unsymmetrical near-IR small molecule with squaraine chromophore for solution processed bulk heterojunction solar cells

Sanghyun Paek,[a] Hyeju Choi,[a] Hyunjun Jo,[a] Kiae Lee,[b] Kihyung Song,[b] S. A. Siddiqui[c], G. D. Sharma,*[d] Jaejung Ko*[a]

[a] Department of Materials Chemistry, Korea University 2511 Sejong-Ro, Sejong 339-700, Republic of Korea. E-mail: jko@korea.ac.kr; Fax: +82-44-867-5396; Tel: +82-44-860-1337
[b] Department of Chemical Education, Korea National University of Education, Chungbuk, 363-791, Republic of Korea.
Department of Electrical Engineering, Vivekanand Institute of Technology (VIT), Jagatpura, Jaipur, Raj, India
[c] R & D Center for Engineering and Science, JEC Group of Colleges, Jaipur Engineering College Campus, Kukas, Jaipur, Raj., India. E-mail: gdsharma273@gmail.com; sharmagd_in@yahoo.com

Abstract

A new unsymmetrical low bandgap push-pull squaraine chromophore bis-DMFA-Th-SQ-Th-DCA denoted as **JK216D** was synthesized and its optical and electrochemical properties (both theoretical and experimental) were investigated. This small molecule having the strong electron withdrawing moiety exhibits broader absorption band in thin film. The **JK216D** exhibited suitable highest occupied molecular orbital (HOMO) and lowest unoccupied molecular orbital energy levels, compatible with that of $PC_{71}BM$, for efficient photoinduced electron transfer. The bulk heterojunction solar cell fabricated with **JK216D**:$PC_{71}BM$ (optimized weight ratio of 1:2 and processed with CB) exhibited a PCE of 3.60% (J_{sc} = 9.97 mA/cm^2, V_{oc}= 0.86V and FF= 0.42). The PCE has been further improved up to 5.25 % (J_{sc} = 11.86 mA/cm^2, V_{oc} = 0.82 and FF= 0.54), when the optimized **JK216D**:$PC_{71}BM$ (1:2) active layer was processed with the addition of 3v% DIO into the CB solution.

Key words: NIR small molecules, bulk heterojunction solar cells, power conversion efficiency and solvent additives

* Corresponding authors

Introduction

Organic bulk heterojunction (BHJ) solar cells have been developing with a quick pace in the past few years due to the number of advantages such as low cost, light weight and large area fabrication on flexible substrates [1]. Among the various organic semiconducting materials used in BHJ organic solar cells (OSCs), an encouraging power conversion efficiency (PCE) about 8-10 % has been achieved by low bandgap conjugated polymers as donor and fullerene derivatives as acceptor in BHJ OSCs [2] through the enormous efforts including device architectures and optimization of device processing. These polymers have potential applications in next generation solar cells and can compete with inorganic solar cells. However, the polydispersity inherent to polymers can represent a possible source of problems regarding the reproducibility of the synthesis, and purification [3].

Meanwhile, solution-processed small molecules as donor materials in bulk heterojunction (BHJ) organic solar cells have attracted considerable interest in recent years due to their well defined structure, reduced batch-to-batch variations, and easier purification or synthesis compared with polymeric donor materials. Since fabrication methods with semiconducting small molecules are more suited to mass production compared to those of polymer based materials. Significant research efforts in recent years have been directed to develop efficient small molecules organic semiconducting materials in an effort to improve the performance of solution processed small molecule BHJ OSCs [4]. Recently, SMOSCs with PCE in the range of 7-10% have been reported after the combination of structural design, morphology control and device engineering [5], thus making solution processed SMOSCs strong competitors to PSCs.

To achieve the high PCE of the SMOSCs, it is necessary to design the small molecule donors with broad absorption profile that matches with the solar spectrum, low optical bandgap and suitable energy levels compatible with the PCBM acceptors. The most commonly reported organic semiconductors for the use in SMOSCs often have push-pull molecular skeletons composed of electron donating groups bridged with electron accepting groups via π-conjugated motifs [6]. The push-pull structure of small molecules enhances the intramolecular charge transfer (ICT), yielding higher molar absorption coefficient in addition to narrow bandgap. In addition, triarylamine groups such as triphenylamine (TPA) and bis(9, 9-dimethyl-9*H*-fluoren-2-yl)aniline (bisDMFA) can play an important role in stabilizing holes dissociated from excitons and thereby improving the transporting in the device. Moreover, chromophore containing squaraine (SQ) moiety have also been developed for

small molecule based solar cell [7] due to their high molar extinction coefficients, intense absorption in NIR region of solar spectrum, excellent photochemical and photophysical stability [8]. The SQ based small molecules used in those devices have a symmetrical molecular structure (D-A-D) [9]. However, asymmetrical SQs (D-A-D') are more promising candidates relative to symmetrical SQ because of their better photo-physical properties [10].

Major factors for the design of small molecules in the organic solar cells are to keep their stability and good morphology, as well as to have broad and red-shifted absorption bands. To incorporate these required properties, we have designed and synthesized the unsymmetrical small molecule **JK216D** that consist of the dimethylfluoreneaniline unit acting as electron donor and alkyl cyanoacetate and squaraine (SQ) moieties as electron acceptor, the two functions being connected by conducting thiophene and pyrrole units. The dimethylfluoreneaniline moiety in **JK216D** ensures greater resistance to degradation when exposed to light and high temperature compared to simple triphenylamine [11]. The moiety is also amorphous, helping to keep good morphology [11a, 12]. The bridging thiophene and pyrrole units are introduced to provide conjugation in order to increase the molar extinction coefficient. The squarine unit was also introduced to obtain the red-shifted and broad UV spectrum. The alkyl cyanoacetate was adapted in the small molecule because of its capability of the intramolecular charge transfer and the facile control of morphology [13].

Herein, we report the synthesis, optical and electrochemical properties of a novel near-IR small molecule; bisDMFA-Th-SQ-Th-DCA denoted as **JK216D** as donor along with PC_{71} BM. We have achieved the PCE of 3.60 % with the optimized **JK216D**:PC_{71}BM active layer processed with CB solvent and further improved up to 5.25% when the active layer was processed with optimized 3 v% DIO solvent additive. The improved PCE has been attributed to the enhancement in J_{sc} and FF.

Experimental details

General Methods: All reactions were carried out under a nitrogen atmosphere. Solvents were distilled from appropriate reagents. All reagents were purchased from Sigma-Aldrich, TCI and Alfa Aesar. ^{1}H and ^{13}C NMR spectra were recorded on a Varian Mercury 300 spectrometer. Elemental analyses were performed with a Carlo Elba Instruments CHNS-OEA 1108 analyzer. Mass spectra were recorded on a JEOL JMS-SX102A instrument. The absorption and photoluminescence spectra were recorded on a Perkin-Elmer Lambda 2S UV-visible spectrometer and a Perkin LS fluorescence spectrometer, respectively.

Cyclic voltammogram: Cyclic voltammetry was carried out with a BAS 100B (Bioanalytical Systems, Inc.). A three electrode system was used and consisted of non-aqueous Reference

Electrode (0.1 M Ag/Ag^+ acetonitrile solution; MF-2062, Bioanalytical System, Inc.), platinum working electrode (MF-2013, Bioanalytical System, Inc.), and a platinum wire (diam. 1.0 mm, 99.9% trace metals basis, Sigma-Aldrich) as counter electrode. Redox potential of dyes was measured in CH_2Cl_2 with 0.1 M $(n\text{-}C_4H_9)_4N\text{-}PF_6$ as a scan rate of 50 mV s^{-1} (vs. Fc/Fc^+ as an external reference).

Synthesis of JK216D

Compound 3: **1** (1 g, 1.3 mmol) and **2** (5-bromo-2,3,3-trimethyl-1-octyl-3H-indolium)(0.6 g 1.3 mmol) were dissolved in a mixture of 60 mL of *n*-propanol and 60 mL of benzene. The mixture was refluxed for overnight. The solvent was removed. The product **3** was obtained by silica gel chromatography (eluent EA :Hx = 1 : 1). MS: *m/z*1066 $[M^+]$.^{1}H NMR($CDCl_3$) (spectra is shown in supporting information) : δ7.72 (d, 1H, ^3J = 4.2 Hz), 7.66 (d, 2H,^3J =6.9 Hz), 7.62 (d, 2H,^3J =8.4 Hz),7.54-7.46 (m, 4H), 7.40 (d, 2H,^3J =7.8 Hz),7.35-7.26 (m, 8H), 7.20 (d, 2H, ^3J =9.3 Hz), 7.13 (dd, 2H, ^3J = 8.4 Hz), 6.94 (d, 1H, ^3J = 8.4 Hz), 6.72 (d, 2H, ^3J =4.2 Hz), 6.09 (s, 1H), 4.42 (s, 3H), 4.05 (t, 2H), 1.81 (m, 8H), 1.44-1.26 (m, 22H), 0.87 (t, 3H).$^{13}C\{^1H\}$ NMR ($CDCl_3$) : δ 184.30, 172.56, 155.31, 153.68, 148.15, 146.98, 146.21, 144.74, 141.12, 139.47, 139.00, 134.77, 131.58, 131.18, 130.59, 128.34, 127.44, 127.16, 126.75, 126.09, 123.63, 123.29, 122.65, 121.29, 120.83, 119.62, 119.10, 118.34, 115.26, 111.78, 89.30, 50.37, 47.01, 44.53, 36.28, 31.82, 29.38, 29.22, 27.40, 27.18, 27.11, 26.83, 22.70, 14.20. Anal. Calc. for $C_{68}H_{64}BrN_3O_2S$:C, 76.53; H, 6.04; N, 3.94. Found : C, 76.33; H, 6.21; N, 4.01.

Compound 4: Compound **3** (1 g, 0.94 mmol), 5-formyl-2-thienylboronic acid (0.22 g, 1.45mmol), $Pd(PPh_3)_4$ (75mg, 0.06mmol), and anhydrous K_2CO_3 (1.29 g, 4.7mmol) were added to a 125 mL flame-dried 2-neck round-bottom flask with a condenser in THF/H_2O under a nitrogen atmosphere. The reaction mixture was heated to reflux for 14 hrs. The reaction mixture was then cooled to room temperature. The organic layer was separated and dried over anhydrous magnesium sulfate. The solvent was removed in *vacuo*. The product was purified by column chromatography (eluent EA :Hx = 1 : 1). MS: *m/z*1097 $[M^+]$.^{1}H NMR($CDCl_3$) (spectra is shown in supporting information) : δ 9.90 (s, 1H), 7.75 (d, 2H, ^3J = 4.2 Hz), 7.71-7.64 (m, 6H), 7.61 (s, 1H), 7.55-7.52 (m, 3H), 7.48-7.39 (m, 5H), 7.34-7.27 (m, 4H), 7.20 (d, 2H, ^3J =7.8 Hz), 7.15-7.11 (m, 3H), 6.74 (d, 1H, ^3J =4.2 Hz) 6.15 (s, 1H), 4.44 (s, 3H), 4.10(m, 2H), 1.87 (m, 8H), 1.42-1.25 (m, 22H), 0.89-0.85 (m, 3H).$^{13}C\{^1H\}$ NMR ($CDCl_3$): δ182.76, 172.44, 155.32, 153.70, 153.52, 152.34, 148.22, 146.97, 146.43, 143.81, 143.07, 142.59, 139.87, 139.00, 137.59, 134.79, 132.31, 132.19, 132.08, 131.49, 130.67, 130.17, 128.72, 128.56, 127.39, 127.18, 126.77, 124.23, 123.67, 123.59, 123.33, 122.66,

121.65, 120.83, 120.54, 119.64, 119.13, 115.45, 110.96, 90.15, 89.73, 50.19, 47.02, 44.57, 36.34, 31.84, 29.41, 29.23, 27.51, 27.19, 26.99, 22.72, 14.20.Anal. Calc. for $C_{73}H_{67}N_3O_3S_2$:C, 79.82; H, 6.15; N, 3.83. Found : C, 79.79; H, 6.41; N, 3.98.

JK216D: Compound **4** (0.5 g,0.45 mmol) and hexylcyanoacetate(1.54 g, 9.0 mmol) was dissolved in dry CH_2Cl_2 and then few drops of triethylamine were stirred for 1 hr under nitrogen at room temperature. The solution was removed. The product was purified by column chromatography (eluent EA :Hx = 1 : 5 and then EA : MC = 1 : 1).MS: *m/z*1247 [M^+]. ^{1}H NMR($CDCl_3$) (spectra is shown in supporting information): δ 8.30 (s, 1H), 7.77-7.75 (m, 2H), 7.72-7.61 (m, 7H), 7.54 (d, 2H, ^3J =9.0 Hz), 7.42 (d, 1H, ^3J =3.6 Hz), 7.42-7.18 (m, 9H), 7.20 (d, 2H, ^3J =9.0 Hz), 7.14-7.09 (m, 3H), 6.74 (d, 1H, ^3J =3.9 Hz) 6.15 (s, 1H), 4.44 (s, 3H), 4.31 (t, 2H), 4.10(m, 2H), 1.87 (m, 10H), 1.42-1.25 (m, 28H), 0.89-0.85 (m, 6H).^{13}C{^{1}H} NMR ($CDCl_3$): δ183.86, 172.33, 155.32, 153.80, 153.70, 148.22, 146.97, 146.50, 146.46, 143.85, 143.23, 139.95, 139.43, 139.00, 135.17, 134.79, 131.47, 130.70, 129.84, 128.53, 127.38, 127.18, 126.77, 124.50, 123.66, 123.57, 123.35, 122.66, 121.75, 120.83, 120.50, 119.64, 119.13, 116.16, 115.49, 111.00, 98.24, 89.83, 66.80, 50.20, 47.01, 36.35, 31.84, 31.52, 29.84, 29.41, 29.23, 28.65, 27.50, 27.18, 25.60, 22.72, 22.65, 14.21, 14.13.Anal. Calc. for $C_{82}H_{80}N_4O_4S_2$:C, 78.81; H, 6.45. Found : C, 78.55; H, 6.61.

The fabrication of the devices and their characterization is given in supporting information.

Results and discussions

Synthesis of JK216D

We prepared new a p-type near-IR organic semiconductor based on squaraine according to the synthetic protocol reported in the Scheme 1. The condensation reaction of **1** with **2** in toluene/isopropanol produced compound **3**. The Suzuki reaction of **3** with 1.2 equivalents of 5-formyl-2-thienylboronic acid yields **4**. **JK-216D** was prepared through Knoevenagel condensation of **4** with hexyl cyanoacrylate. Additional details are given in the Experimental Section (supporting information).

Optical and electrochemical properties

Figure 1 shows the UV-visible absorption spectra of **JK216D** in chlorobenzene (CB) solution and thin film cast from CB solvent, and corresponding optical properties are summarized in Table 1. As shown in Figure 1 (black line), the absorption spectra of **JK216D** in CB showed a sharp absorption in longer wavelength region 600 -800 nm with a high molar absorption coefficient of 119,000 M^{-1} cm^{-1} at 720 nm. This high molar extinction coefficient may be caused by the stronger intramolecular charge transfer (ICT) from bis-DMFA to squaraine core. The film casted from the CB solvent exhibited the broaden spectrum up to

900 nm, but the maximum absorption peak was red-shifted by around 16 nm, showing the absorption to the NIR. The red-shift and broadening of absorption band in the longer wavelength region was attributed to the presence of intermolecular interactions and aggregation of small molecule in solid state. The optical bandgap estimated from onset absorption edge is about 1.48 eV.

In order to determine the redox behavior of **JK216D** and determine its HOMO and LUMO energy levels, we have investigated the cyclic voltammetry (CV) of **JK216D** in solid state and shown in Figure 2(a) (oxidation cyclic). The electrochemical parameters are summarized in table 1. The HOMO energy level can be deduced from the oxidation onset with the assumption that the energy level of ferrocene is 4.8 eV below vacuum level. But the reduction potential of **JK216D** was not clearly observed in cyclic voltammogram. Therefore, we have determined the $E_{o\text{-}o}$ transition energy from the intersection of absorption and emission spectra of **JK216D** in solution (Figure 2b). The HOMO energy level of the **JK216D**, estimated from the onset oxidation potential observed in CV was -5.086 eV. The deeper energy is beneficial for the high value of V_{oc}, when used as donor for the fabrication of BHJ solar cells along with $PC_{71}BM$ as electron acceptor. The LUMO energy level was estimated according $E_{LUMO} = E_{HOMO} - E_{o\text{-}o}$ and was about -3.436 eV. In general, an exciton dissociation and efficient electron transfer from the donor to the acceptor molecule requires a higher LUMO level of donor by at least ~0.3 eV to the LUMO energy level of acceptor molecule [14]. The LUMO level of the $PC_{71}BM$ has values in the range between 3.9 eV to 4.1 eV [15]. In our case, the LUMO-LUMO offset between the **JK216D** and $PC_{71}BM$ is larger than ~0.3 eV, therefore, it could be expected that exciton might easily dissociate at the donor –acceptor interface formed in the BHJ active layer.

DFT calculations

The electronic properties of **JK-216D** have also been investigated through theoretical calculations. Figure 3 shows the optimized structures of **JK-216D** (for details, see Table 2), which were calculated by TD-DFT using the B3LYP functional/6-31G* basis set. The orbital density of the HOMO and HOMO-1 of **JK-216D** was bis-DMFA-thiophene-pyrrol core owing to its greater electron-donating strength, whereas the orbital density of LUMO and LUMO+1 was predominantly located between the squaraine and cyanoacrylate unit. These results indicate that the ICT of **JK-216D** was efficiently demonstrated between bis-DMFA-thiophene-pyrrol (HOMO, HOMO-1) and squaraine-cyanoacrylate (LUMO, LUMO+1) unit.

Photovoltaic properties

In BHJ organic solar cells, the relative amounts of the donor and acceptor materials used in the active layer play an important role for efficient photovoltaic performance, since there should be balance between the absorbance and charge transporting network of active layer. When the acceptor content is too low, the electron transporting ability will be limited, while when the acceptor content is too high, the absorbance and hole transport ability in the active layer will be decreased. BHJ active layers with a blend of **JK216D** and $PC_{71}BM$ in CB in different weight ratio were investigated and the optimized blend ratio was found to be 1:2, for which we observed highest photovoltaic performance. We have only discussed our results only for this blend ratio.

Figure 4 shows the UV-visible absorption spectra of **JK216D**:$PC_{71}BM$ (1:2) film casted from CB (black color). As shown in Figure 4 the absorption band of **JK216D** in the **JK216D**:$PC_{71}BM$ blend deposited from CB was blue shifted by 18 nm compared to that of its pristine films in Figure 1, but extended up to 900 nm. Moreover, the absorption spectra of the blend showed the combination of both PC71BM and **JK216D**, indicating that both components used in the active layer might contribute to the exciton generation and thereby photocurrent generation.

The Photoluminescence (PL) spectroscopy of the blend was measured to investigate the exciton separation efficiency. The PL spectra of **JK216D** and **JK216D**:$PC_{71}BM$ are shown in Figure 5. It can be seen from this Figure that the pristine **JK216D** showed a strong emission peak at 772 nm, which might reduce the possibility of charge recombination in film state, and hence induces the exciton diffusion towards the donor-acceptor interface, which is ultimately beneficial for exciton dissociation [16], while when **JK216D** blended with $PC_{71}BM$, this emission peak is significantly quenched and the quenching is more effective with DIO/CB. This effective PL quenching suggested that the excitons generated by the absorbing the photons would dissociate to free charge carrier (electrons and holes) effectively. Thus, effective charge transfer from **JK216D** donor to $PC_{71}BM$ acceptor took place [17].

The current-voltage (J-V) characteristics of BHJ organic solar cells, under stimulated (AM1.5, 100 mW/cm^2) with **JK216D**:$PC_{71}BM$ (1:2) spin cast from CB solution is displayed in Figure 6a (black color) and corresponding photovoltaic parameters are complied in Table 2. The device showed an overall PCE of 3.60 % with J_{sc} = 9.97 mA/cm^2, V_{oc} = 0.86 V and FF = 0.42. This PCE is higher than the small molecule bis[DMFA-Th]-DiF-BT-HxTh3, reported

earlier by us [18]. It may be due to the broader absorption profile of **JK216D** compared to bis[DMFA-Th]-DiF-BT-HxTh3, due to more exciton generation, leading to higher J_{sc}.

The incident photon to current conversion efficiency (IPCE) values were estimated from the expression

$$IPCE\ (\lambda) = 1240\ J_{sc}/\lambda P_{in}$$

where J_{sc} is the photocurrent under short circuit conditions, and λ and P_{in} are the incident photon flux and wavelength of incident monochromatic light, respectively. The IPCE spectrum (Figure 6b, black line) of the device closely resembles with the absorption spectrum of the active layer, indicating that both the **JK216D** and **$PC_{71}BM$** contribute to the exciton generation, thereby generating photocurrent generation.

The overall PCE of solar cells based on **JK216D**:$PC_{71}BM$ blend active layer processed from the CB solvent is considered to be low, compared to the latest development on polymer and some small molecules. Although, the V_{oc} of the organic solar cell fabricated with **JK216D**:$PC_{71}BM$ processed with CB is quite high, its poor PCE is attributed to the low values of J_{sc} and FF. These values are directly related to the light harvesting efficiency of active layer, morphology of active layer, charge transport and their collection to the respective electrodes. Since in BHJ organic solar cells, the J_{sc} value is determined by the transportation rate of both electron and hole within the active layer towards the respective electrodes, i.e. electrons and holes towards the cathode and anode, respectively. Generally, the electron mobility is much higher than the hole mobility, resulting a unbalanced charge transport. It leads to the formation of space charge at the anode and recombination loss of charge carriers within the active layer before reaching to the electrodes. Moreover, for efficient organic BHJ solar cells, the active layer morphology should have an interpenetrating network of donor and acceptor materials with domain sizes on the order of exciton diffusion length or around 10-20 nm [19]. Moreover, the active layer should have enough interfacial area to dissociate all the excitons generated in the active layer, while also maintaining continuous charge transport pathways to the electrodes. Therefore, appropriate nanoscale morphology of active layer is necessary to both above processes for efficient organic solar cell. In general, the typical parameters that affect the morphology of active layer include the solvent, donor/acceptor concentrations, thermal annealing times and temperature, solvent annealing conditions, solvent additives and the interlayer surface energies [20-22].

In an effort to improve the performance of the BHJ organic solar cell based on **JK216D**:$PC_{71}BM$ (1:2) active layer, we have used solvent additive method and cast the

active layer from the optimized concentration of 3 v% mixture of DIO in CB. The J-V characteristics of the resulting device are shown in Figure 6a (red line) and corresponding photovoltaic parameters are complied in table 2. The PCE value of the device was improved from 3.60 % to 5.25 % (J_{sc} =11.86 mA/cm^2, V_{oc} =0.82 V and FF= 0.54). The changes in the properties such as film morphology and hole mobility will be discussed latter part of the discussion.

The enhancement in the overall PCE of the latter device is attributed to its increased J_{sc} (from 9.97 mA/cm^2 to 11.86 mA/cm^2) and FF (from 0.42 to 0.54) values. In order to investigate the effect of solvent additive (DIO) on the device performance, UV-visible absorption spectra of blend films and IPCE were measured. As shown in Figure 3 (red color), in comparison with the spectra of the blend cast from CB solvent, the spectra of film processed with DIO/CB showed enhanced absorption coefficient, particularly in the near-IR region. The increase in the J_{sc} value is ascribed to the higher values of IPCE (Figure 6b, red color) and broader response of the latter solar cell compared to the former cell [23]. The calculated J_{sc} obtained from the integration of the IPCE curves are about 9.86 mA/cm^2 and 11.74 mA/cm^2 for devices processed with CB and DIO/CB, respectively. These values are consistent with the values experimentally observed from the J-V characteristics. Moreover, as can be seen from the Figure 4 that the PL emission is significantly quenched when the **JK216D**:$PC_{71}BM$ blend cast from DIO/CB solvent, the exciton separation is more effective in this active layer compared to that of the film processed with CB solution. The more effective quenching in the BHJ active layer processed with DIO/CB compared to CB implies two possibilities: (i) better exciton separation in the active layer, and (ii) a larger contact area between **JK216D** and $PC_{71}BM$ through more optimal nanoscale phase separation. The former could be ruled out because the same donor and acceptor were used in the both active layer. The latter was thus mainly responsible for effective PL quenching, as confirmed from the film morphology studies and will be discussed in the following discussion.

The performances of organic solar cells using a BHJ active layer are closely related to its morphology. Therefore, we have investigated the film morphologies of **JK216D**:$PC_{71}BM$ (cast from CB and DIO/CB in optimized active layers) by performing tapping mode atomic force microscopy (AFM). Figure 7 shows the AFM height images of active layer films spun cast from CB and DIO/CB solvents. It is well known that smooth morphology and homogenous blend with the nanophase separation are responsible for the large donor–acceptor interface area needed for exciton dissociation [24]. The BHJ active **JK216D**:$PC_{71}BM$ layer film processed with CB (Figure 6a) is relatively homogenous and

nearly flat surface with root mean squared (rms) roughness of 0.64 nm. But it does not showed much phase separated surfaces, indicating that flat surface does not provide the sufficient D-A interfaces for exciton dissociation as well pathways for charge transport, leading to the low value of J_{sc}. However, the film cast from DIO/CB showed more aggregated domains and phase separated surface with larger rms roughness of 1.98 nm. The larger domains are most likely originated from the enhancements in the intermolecular interactions of **JK216D** [25]. The higher roughness of the active layer processed with DIO/CB indicates that this film exhibits reduced internal resistance and more efficient charge separation in the device [26]. A higher surface roughness also leads to increased internal light scattering and enhanced light absorption [27], as confirmed from the absorption spectra of active layer (Figure 3). The proper homogeneity and phase separated domain sizes of **JK216D** and $PC_{71}BM$ in the blend layer provide enough surface area for exciton dissociation and bicontinuous network, which acts as percolation channels for efficient carrier collection within the active layer of BHJ solar cells [28]. These effects leads to increase the J_{sc} and over all PCE of the device.

The low FF value of the device processed from the CB solvent is due to the number of reasons such as domain size, morphology and series resistance. The series resistance is composed of resistance of the active layer of the device in addition to the resistance of different interfaces. The low FF is related to the increase in the series resistance of **JK216D**:$PC_{71}BM$/PEDOT:PSS/ITO, resulting in high recombination rate [29]. The high FF of device with **JK216D**:$PC_{71}BM$ processed with DIO/CB is related to its low series resistance of ~5.34 Ω cm^2 compared to that for CB processed device with high series resistance of ~8.23 Ω cm^2.

In BHJ solar cells, the electron and hole mobilities of donor and acceptor materials play a crucial role, as these should be balanced in order to achieve an efficient charge transport. The hole (μ_h) and electron (μ_e) mobilities of **JK216D** and $PC_{71}BM$ in the blended active layers were estimated from the hole only device and electron only devices from the space charge limited current (SCLC) J-V characteristics in dark [30]. Figure 8 shows dark J-V characteristics of hole only devices processed with CB and DIO/CB solvents. The bias voltage was corrected for the built in voltage determined from the difference between the work functions of Au and PEDOT:PSS. Similar J-V characteristics were observed for electron only devices. The SCLC behavior of J-V characteristics cab be expressed by Mott-Gurney square law:

$J = 9/8\ \varepsilon\mu(V^2/L^3)$

where ε is the static dielectric constant of the medium, μ is the carrier mobility, V is the applied bias voltage corrected with the built in potential, and L is the thickness of the active layer. The average μ_h and μ_e are 1.68×10^{-5} cm^2/Vs and 2.48×10^{-5} cm^2/Vs, respectively for the devices using above Mott- Gurney law in the **JK216D**:$PC_{71}BM$ active layers processed with CB solvent. However, when the active layer was processed with DIO/CB, the average μ_h and μ_e are 5.72×10^{-5} cm^2/Vs and 2.42×10^{-5} cm^2/Vs, respectively. The μ_h of the device processed with DIO/CB is higher than that of the device processed with CB. This difference is closely related to intermolecular packing interactions, enhanced exciton separation efficiency, and charge transport [31]. The increase in the μ_h, reduces the ratio between μ_e and μ_h in the active layer from 14.76 (for CB processed) to 4.12 (DIO/CB processed), enhancing the J_{sc} and FF and overall PCE [32].

Conclusion

We have demonstrated the synthesis, optical and electrochemical properties of a new small molecule **JK216D**. The electrochemical energy levels **JK216D** are compatible with the $PC_{71}BM$ for efficient exciton dissociations and charge separation. The solution processed BHJ organic solar cell fabricated from the blend thin film of **JK216D** as donor and $PC_{71}BM$ as acceptor in the optimized weight ratio of 1:2 (CB cast) showed a PCE of 3.60% with J_{sc} = 9.97 mA/cm^2, V_{oc} = 0.86 V and FF= 0.42. In order to improve further the PCE of organic solar cell, the **JK126D**:$PC_{71}BM$ active layer was spin cast from a mixture of 3v% DIO/CB. The device showed PCE of 5.25 % that was attributed to the enhancement in the J_{sc} (11.86 mA/cm^2) and FF (0.54). The enhancement in J_{sc} and FF is related to the more appropriate phase separated nanomorphology and improved balance charge transport. Since the blend **JK216D**:$PC_{71}BM$ exhibited a broad absorption profile, the PCE of the organic solar cell using this blend can be further improved by employing the appropriate electron and hole transporting layers. This work is in progress.

Acknowledgements

This research was supported by the International Science and Business Belt Program (2013K000496) and the ERC (the Korean government (MEST)) program (2013004800) through the Ministry of Science, ICT and Future Planning. GDS thankful to the management, JEC group of colleges, Jaipur Engineering college, Jaipur for providing necessary facilities.

We are also thankful to LNMIIT, Jaipur for proving the facilities for device fabrication and characterization.

References

1. (a) G. Yu, J. Gao, J. C. Hummelen, F. Wudl and A. J. Heeger, *Science*, 1995, **270**, 1789-1791; (b) Y. J. Cheng, S. H. Yang and C. S. Hsu, *Chem. Rev*., 2009, **109**, 5868 (c) F. C. Krebs, *Sol. Energy Mater. Sol. Cells* 2009, **93**, 394-412; (d) A. C. Arias, J. D. Mackenzie, I. McCulloch, J. Rivnay and A. Salleo, *Chem. Rev*. 2010, 110, 3-24; (e) T. D. Nielsen, C. Cruickshank, S. Foged, J. Thorsen and F. C. Kreb, *Sol. Energy Mater. Sol. Cells* 2010, **94**, 1553-1571; (f) H. Hoppe and N. S. Sariciftci, *J. Mater. Chem.* 2006, **16**, 45-61; (g) M. Helgesen, R. Søndergaard and F. C. Krebs, *J. Mater. Chem.* 2010, **20**, 36-60; (h) W. Cao and J. Xue, *Energy Environ. Sci.*, 2014, **7**, 2123–2144

2. (a) Z. C. He, C. M. Zhong, S. J. Su, M. Xu, H.B. Wu and Y. Cao, *Nat. Photonics*, 2012, **6**, 593-597; (b) W. Y. Wong and C and L. Ho *Acc. Chem. Res*., 2010, **43**, 1246; (c) Z. C. He, C. M. Zhong, X. Huang, W.-Y. Wong, H. B. Wu, L. W. Chen, S. J. Su and Y. Cao, *Adv. Mater*., 2011, **23**, 4636; (d) J. Yo, L. Dou, K. Yoshimura, T. Kato, K. Ohya, T. Moriarty, K. Emery, C. C. Chen, J. Gao, G. Li and Y. Yang, *Nat. Commun*., 2013, **4**, 1446; (e) S. Liu , K. Zhang , J. Lu , J. Zhang , H.-L. Yip , F. Huang and Y. Cao, *J. Am. Chem. Soc.* 2013, **135**, 15326

3. W. Li, L. Yang, J. R. Tumbleston, L. Yan, H. Ade and W. You, *Adv Mater*., 2014, **26**, 4456

4. (a) Z. He, C. Zhong, S. Su, M. Xu, H. Wu and Y. Cao, *Nat. Photonics* 2012, **6**, 593−597; (b) J. Roncali, *Acc. Chem. Res*., 2009, **42**, 1719−1730, (c) D. Demeter, T. Rousseau, P. Leriche, T. Cauchy, R. Po, and J. Roncali, *Adv. Funct. Mater*., 2011, **21**, 4379−4387; (d) Y. Sun, G. C. Welch, W. L. Leong, C. J. Takacs, G. C. Bazan, and A. J. Heeger, *Nat. Mater*., 2012, **11**, 44−48; (e) A. Mishra and P. Buerle, *Angew. Chem. Int. Ed*., 2012, **51**, 2020– 2067; (f) Y. Lin, Y. Li and X. Zhan, *Chem. Soc. Rev*. 2012, **41**, 4245; (g) J. E. Coughlin, Z. B. Henson, G.C. Welch and G.C. Bazan, *Acc. Chem. Res*. 2014, **47**, 257

5. (a) Q. Zhang, B. Kan, F. Liu, G. Long, X. Wan, X. Chen, Y. Zuo, W. Ni, H. Zhang, M. Li, Z. Hu, F. Huang, Y. Cao, Z. Liang, M. Zhang, T. P. Russel, Y. Chen, *Nat. photonics* doi: 10.1038/NPHOTON.2014.269; (b) J. Zhou, et al. J. Am. Chem. Soc., 2013, **135**, 8484–8487; (c) A.K.K. Kyaw, et al Nano Lett. 2013, 13, 3796–3801; (d) Y. Liu, et al., *Sci. Rep*. 2013, 3, 3356; (e) A. K. K. Kyaw, et al, Adv. Mater. 2013, **25**, 2397–2402

6. (a) Y. Y. Lai, J. M. Yeh, C.E. Tsai and Y.J. Cheng, *Eur. J. Org. Chem*., 2013, 5076-5084; (b) J. Zhou, Y. Zuo, X. Wan, G. Long, Q. Zhang, W. Ni, Y. Liu, Z. Li, G. He, C. Li, B. Kan, M. Li and Y. Chen, *J. Am. Chem. Soc*. 2013, **135**, 8484-8487

7. (a) G. Wei, X. Xiao, S. Wang, K. Sun, K. J. Bergemann, M. E. Tompson and S. R. Forrest, *ACS Nano*, 2012, **6**, 972; (b) S. L. Lam, X. Liu, F. Zhao, C. L. K. Lee and W. L. Kwan, *Chem. Commun*., 2013, **49**, 4543; (c) J. S. Huang, T. Goh, X. Li, M. Y. Sfeir, E. A. Bielinski, S. Tomasulo, M. L. Lee, N. Hazari and A. D. Taylor, *Nat. Photonics*, 2013, **7**, 479; (d) G. Chen, H. Sasabe, Y. Sasaki, H. Katagiri, X.-F. Wang, T.Sano, Z. Hong, Y. Yang and J. Kido, *Chem. Mater*., 2014, **26**, 1356

8. L. Beverina and P. Salice, *Eur. J. Org. Chem*., 2010, 1207

9. G. Wei, S. Wang, K. Sun, M. E. Thompson and S. R. Forrest, *Adv. Energy Mater*., 2011, **1**, 184

10. (a) S. S. Pandey, R. Watanabe, N. Fujikawa, Y. Ogomi, Y. Yamaguchi and S. Hayase, *Proc. SPIE*, 2011, 8111; (b) J. Fabian, *Chem. Rev*., 1992, **92**, 1197; (c) D. Yang, Q. Yang, L. Yang, Q. Luo, Y. Huang, Z. Lu and S. Zhao, *Chem. Commun*., 2013, **49**, 10465; (d) D. Yang, Q. Yang, L. Yang, Q. Luo, Y. Chen, Y. Zhu, Y. Huang, Z. Lu and S. Zhao, *Chem. Commun*. 2014, **50**, 9346-9348

11. (a) Y. Shirota, M. Kinoshita, T. Noda, K. Okumoto, T. Ohara, *J. Am. Chem. Soc*. 2000, **122**, 11021; (b) S. Paek, H. Choi, C. Kim, N. Cho, S. So, K. Song, M. K. Nazeeruddin and J. Ko, *Chem. Commun*., 2011, **47**, 2874.

12. (a) Y. Shirota and H. Kageyama, *Chem. Rev*. 2007, **107**, 953;

13. (a) G. He, Z. Li, X. Wan, Y. Liu, J. Zhou, G. Long, M. Zhang and Y. Chen, *J. Mater. Chem*., 2012, **22**, 9173-9180; (b) Z. Li, G. He, X. Wan, Y. Liu, J. Zhou, G. Long, Y. Zuo, M. Zhang and Y. Chen, *Adv. Energy Mater*., 2012, **2**, 74−77; (c) Y. Liu, X. Wan, F. Wang, J. Zhou, G. Long, J. Tian and Y. Chen, *Adv. Mater*. 2011, **23**, 5387−5391; (d) Y. Liu, X. Wan, F. Wang, J. Zhou, G. Long, J. Tian, J. You, Y. Yang, and Y. Chen, *Adv. Energy Mater*., 2011, **1**, 771−775; (e) J. Zhou, X. Wan, Y. Liu, Y. Zuo, Z. Li, G. He, G. Long, W. Ni, C. Li, X. Su and Y. Chen, *J. Am. Chem. Soc*. 2012, **134**, 16345−16351; (f) H. Bai, Y. Wang, P. Cheng, Y. Li, D. Zhu and X. Zhan, *ACS Appl. Mater. Interfaces* doi: 10.1021/am501316y

14. (a) C. J. Brabec, C. Winder, N. S. Sariciftci, J. C. Hummelen, A. Dhanabalan, P.A. van Hal and R. A. J. Janssen, *Adv. Funct. Mater*., 2002, **12**, 709−712, (b) G. Zhao, G. Wu, C. He, F. Q. Bai, H. Xi, H. X. Zhang and Y. Li, *J. Phys. Chem. C*, 2009, **113**, 2636

15. R. Zhou, Q. D. Li, X. C. Li, S. M. Lu, L. P. Wang, C. H. Zhang, J. Huang, P. Chen, F. Li, X. H. Zhu, W. C. H. Choy, J. Peng, Y. Cao and X. Gong, *Dyes Pigm*., 2014, **101**, 51

16. (a) L. Huo, X. Guo, Y. Li and J. Hou, *Chem. Commun*., 2011, **47**, 8850; (b) P. Dutta, W. Yang, S. H. Eom and S. H. Lee, *Org. Electron*., 2012, **13**, 273; (c) M. Nazim, S. Ameen, M. S. Akhtar, H. K. Seo and H. S. Shin, *RSC Adv*. 2015, **5**, 6286

17. (a) S. W. Shelton, T. L. Chen, D. E. Barclay and B. Ma, *ACS Appl. Mater. Interfaces*, 2012, **4**, 2534; (b) T. Ameri, P. Khoram, J. Min and C. J. Brabec, *Adv. Mater*., 2013, **25**, 4245

18. S. Paek, N. Cho, K. Song, M. J. Jun, J. K. Lee and J. Ko, *J. Phys. Chem. C* 2012, **116**, 23205−23213

19. (a) D. E. Markov, E. Amsterdam, P. W. M. Blom, A. B. Sieval and J. C. Hummelen, *J. Phys. Chem. A* 2005, **109**, 5266-5274; (b) M. Sim, J. Shin, C. Shim, M. Kim, S. B. Jo, J. H. Kim and K. Cho, *J. Phys. Chem. C* 2014, **118**, 760-766

20. (a) J. E. Slota, X. He and W. T. S. Huck, *Nano Today* 2010, **5**, 231; (b) J. Peet, M. L. Senatore, A.J. Heeger and G. C. Bazan, *Adv. Mater*. 2009, **21**, 1521

21. (a) J. K. Lee, W. L. Ma, C. J. Brabec, J. Yuen, J. S. Moon, J. Y. Kim, K. Lee, G.C. Bazan and A. J. Heeger, *J. Am. Chem. Soc*. 2008, **130**, 3619; (b) H. Y. Chen, J. H. Hou, S. Q. Zhang, Y. Y. Liang, G. W. Yang, Y. Yang, L. P. Yu, Y. Wu and G. Li, *Nat. Photonics* 2009, **3**, 649; (c) T. Y. Chu, J. Lu, S. Beaupre, Y. Zhang, J. R. Pouliot, S. Wakim, J. Zhou, M. Leclerc, Z. Li, J. Ding and Y. Tao, *J. Am. Chem. Soc*. 2011, **133**, 4250; (d) Y. Liang, Z. Xu, J. Xia, S. T. Tsai, Y. Wu, G. Li, C. Ray and L. Yu, *Adv. Mater*. 2010, **22**, E135; (e) J. M. Szarko, J. C. Guo, Y. Y. Liang, B. Lee, B. S. Rolczynski, J. Strzalka, T. Xu, S. Loser, T. J. Marks, L. P. Yu and L. X. Chen, *Adv. Mater*. 2010, **22**, 5468; (f) R. C. Coffin, J. Peet, J. Rogers and G.C. Bazan, *Nat. Chem*. 2009, **1**, 657

22. L. A. Perez, J. T. Rogers, M. A. Brady, Y. Sun, G. C. Welch, K. Schmidt, M. F. Toney, H. Jinnai, A. J. Heeger, M. L. Chabinyc, G. C. Bazan and E. J. Kramer, *Chem. Mater*. doi: 10.1021/cm5031987

23. T. S. van der Poll, J. A. Love, T.-Q. Nguyen and G. C. Bazan, *Adv. Mater*., 2012, **24**, 3646.

24. K. Takemoto, M. Karasawa and M. Kimura, *ACS Appl. Mater. Interfaces*, 2012, **4**, 6289

25. Q. Shi, P. Cheng, Y. Li and X. Zhan, *Adv. Energy Mater*., 2012, **2**, 63.

26. Q. Peng, X. Liu, Y. Qin, D. Zhou and J. Xu, *J. Polym. Sci., Part A: Polym. Chem*., 2011, **49**, 4458

27. J. D. Zimmerman, X. Xiao, C. K. Renshaw, S. Wang, V. V. Diev, M. E. Thompson and S. R. Forrest, *Nano Lett*., 2012, **12**, 4366

28. T. W. Holcombe, C. H. Woo, D. F. J. Kavulak, B. C. Thompson and J. M. J. Frechet, *J. Am. Chem. Soc*., 2009, **131**, 14160

29. (a) Y. Li, Q. Guo, Z. Li, J. Pei and W. Tian, *Energy Environ. Sci*., 2010, **3**, 1427; (b) J. S. Moon, C. J. Takacs, S. Cho, R. C. Coffin, H. Kim, G. C. Bazan and A. J. Heeger, *Nano Lett*., 2010, **10**, 4005

30. (a) G. Malliaras, J. Salem, P. Brock and C. Scott, *Phys. Rev. B: Condens. Mater. Phys*., 1998, **58**, 13411, (b) V. D. Mihailetchi, H. Xie, B. de Boer, L. J. A. Koster and P. W. M. Blom, *Adv. Funct. Mater*., 2006, **16**, 699

31. R. Shivanna, S. Shoaee, S. Dimitrov, S. K. Kandappa, S. Rajaram, J. R. Durrant and K. S. Narayan, *Energy Environ. Sci*., 2014, **7**, 435

32. (a) W. Wien, L. Ying, B. B. Y. Hsu, Y. Zhang, T. Q. Ngyuen and G. C. Bazan, *Chem. Commun*. 2013, **49**, 7192; (b) J. Min, Y. N. Luponosov, A. Geri, M. S. Polinskaya, S. M. Peregudova, P. V. Dmitryakov, A. V. Bakirov, M. A. Shcherbina, S. N. Chvalun, S. Grigorian, N. Kaush-Busies, S. A. Ponomarenko, T. Ameri and C. J. Brabec, *Adv. Energy Mater*. 2014, **4**, 1301234

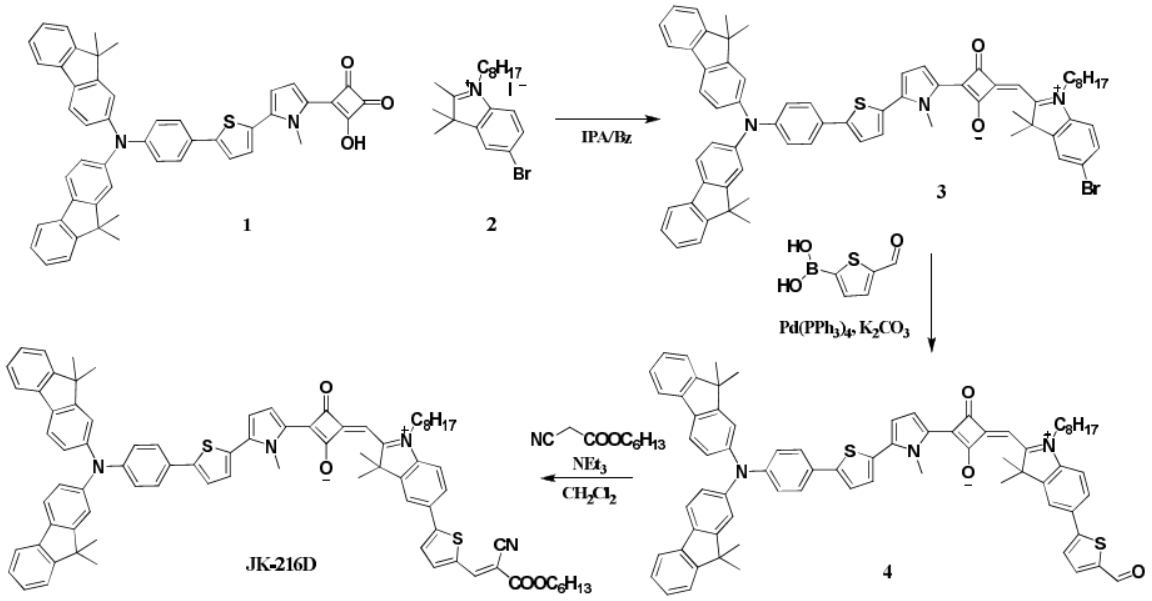

Scheme 1. Schematic diagram for the synthesis of the **JK-216D** small molecule

Table 1 Optical, redox parameters of the **JK-216D**

Compound	λ_{abs}[a]/nm (ε/$M^{-1}cm^{-1}$)	λ_{PL}[a]/nm	E^{ox}_{onset} (V) / E_{HOMO} (eV)[b]	E^{red}_{onset} (V) / LUMO (eV)[b]	$E_{o\text{-}o}$ (eV)[c]	E^{opt}_{g} (eV)[d]
JK216D	378(59,000),720 (119,000)	772	0.206/-5.086	1.444/-3.436	1.65	1.51 eV

[a]Absorption and emission spectra were measured in chlorobezene solution. [b] Redox potential of the compounds were measured in CH_2Cl_2 with 0.1M $(n\text{-}C_4H_9)_4NPF_6$ with a scan rate of 50 mVs^{-1} (*vs.* Fc/Fc^+). [c] $E_{o\text{-}o}$ was calculated from the absorption and emission cross peak in chlorobezene solution. [d] E^{opt}_{g} was calculated from the onset absorption edge of absorption spectra in thin film.

Table 2 Calculated excitation energy characteristics of the **JK-216D**[a]

Compound	E(eV)/nm	f[b]	Composition (%)[c]
JK216D	2.010/616.63	0.106	48 (HOMO-1 → LUMO) 50 (HOMO → LUMO+1)
	2.094/591.91	1.098	49 (HOMO-1 → LUMO)
	2.399/516.74	0.134	68 (HOMO-2 → LUMO+1)

[a] The characteristics were calculated by the time dependent-density functional theory (TD-DFT) using the B3LYP functional/6-31G* basis set

[b] The oscillator strength (*f*) of a transition is a measure of its intensity and is related to the molar absorption coefficient

[c]The composition means contribution of each transition for excitation energies.

Table 3 Photovoltaic parameters of BHJ organic solar cells using **JK216D**:$PC_{71}BM$ (1:2) processed with CB and DIO (3 v%)/CB solvents

Solvent	J_{sc} (mA/cm^2)	V_{oc} (V)	FF	PCE (%)[a]/PCE (%)[b]	Hole mobility (μ_h) (cm^2/Vs)	μ_e/μ_h
CB	9.97	0.86	0.42	3.60a/ 3.54[b]	1.68×10^{-5}	14.76
DIO (3v%)/CB	11.86	0.82	0.54	5.25[a]/5.46[b]	5.72×10^{-5}	4.12

[a] best device
[b]average of 10 devices

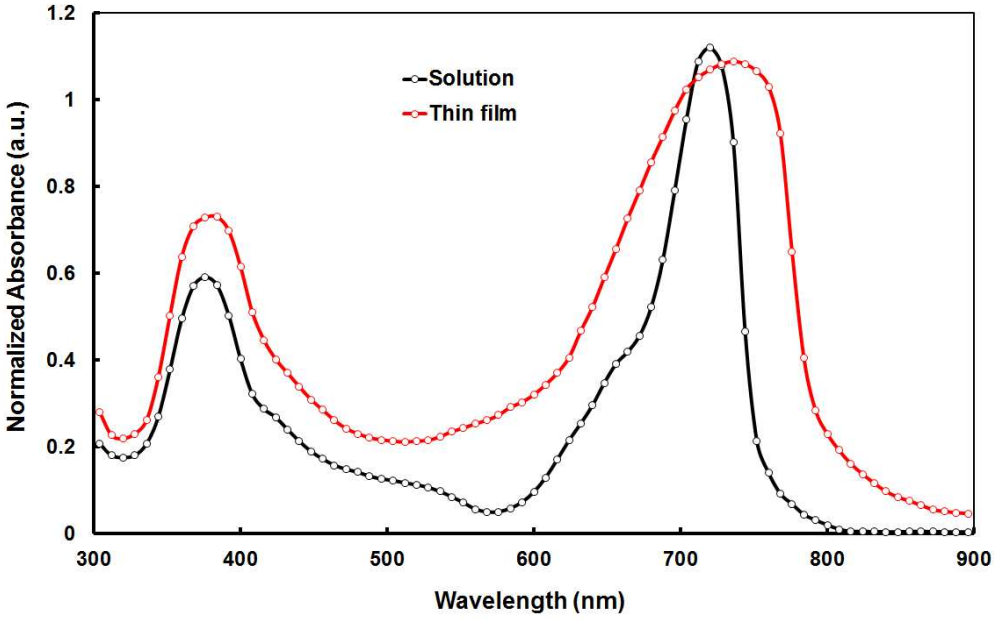

Figure 1 UV-visible absorption spectra of **JK216D** in chlorobenzene solution (black color) and thin film cast from CB (red color)

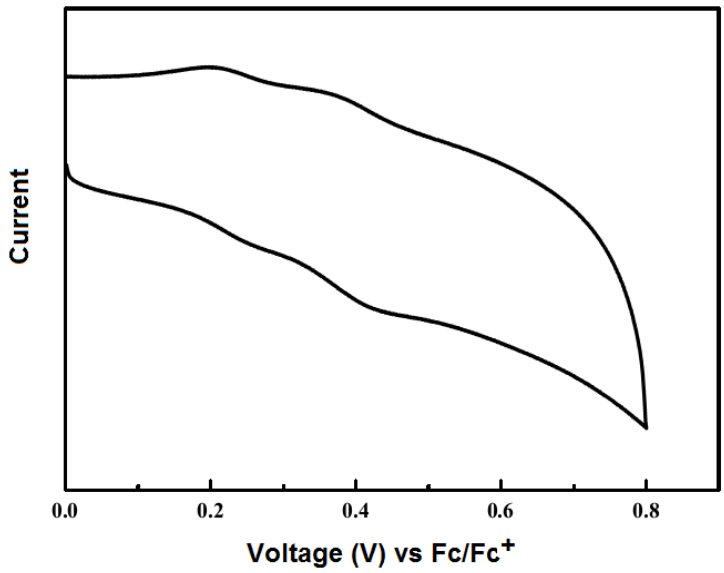

Figure 2 (a) Electrochemical characterization (oxidation) of the **JK216D** 0.1 M tetrabutyl ammonium hexa-fluoro-phosphate in CH_2Cl_2 at scan speed 50 mV/s, potentials vs. Fc/Fc^+

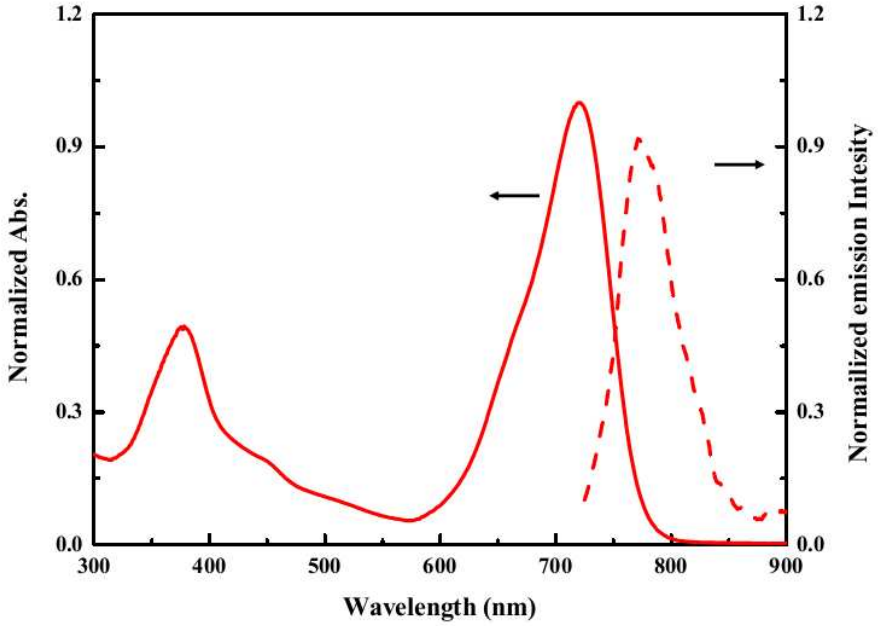

Figure 2b Normalized absorption and emission spectra of **JK-216D** in solution

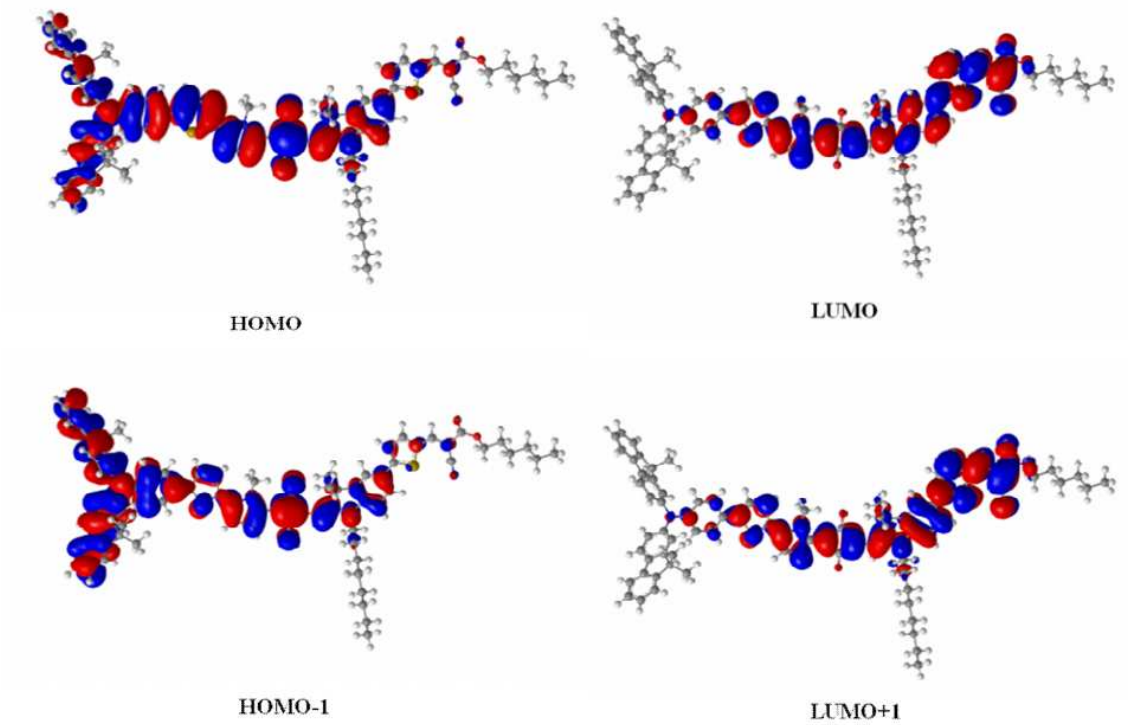

Figure 3 Iso-density surface plots of **JK-216D** calculated by the time dependent-density functional theory (TD-DFT) using the B3LYPfunctional/6-31G* basis set.

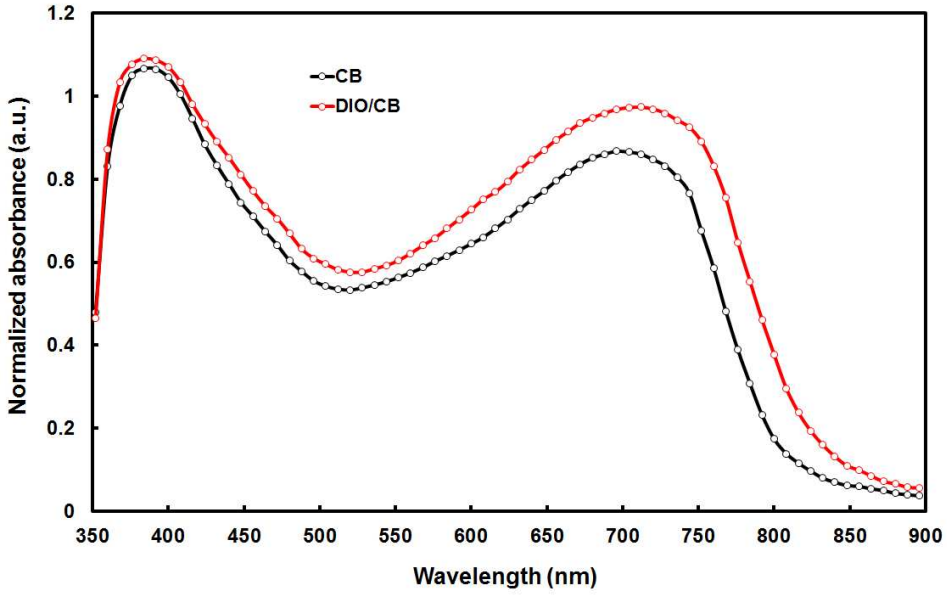

Figure 4 UV-visible absorption spectra of **JK216D**:$PC_{71}BM$ (1:2) films spin cast from the CB and DIO (3v%)/CB solvents.

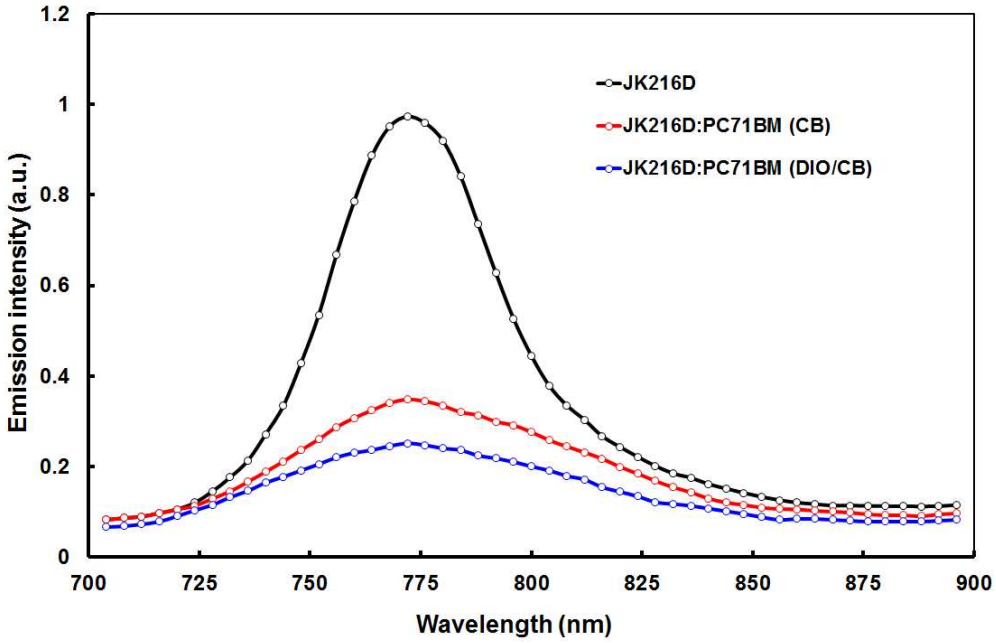

Figure 5 PL spectra of the pristine **JK216D** (CB) and **JK216D**:$PC_{71}BM$ in CB and DIO (3v%) /CB

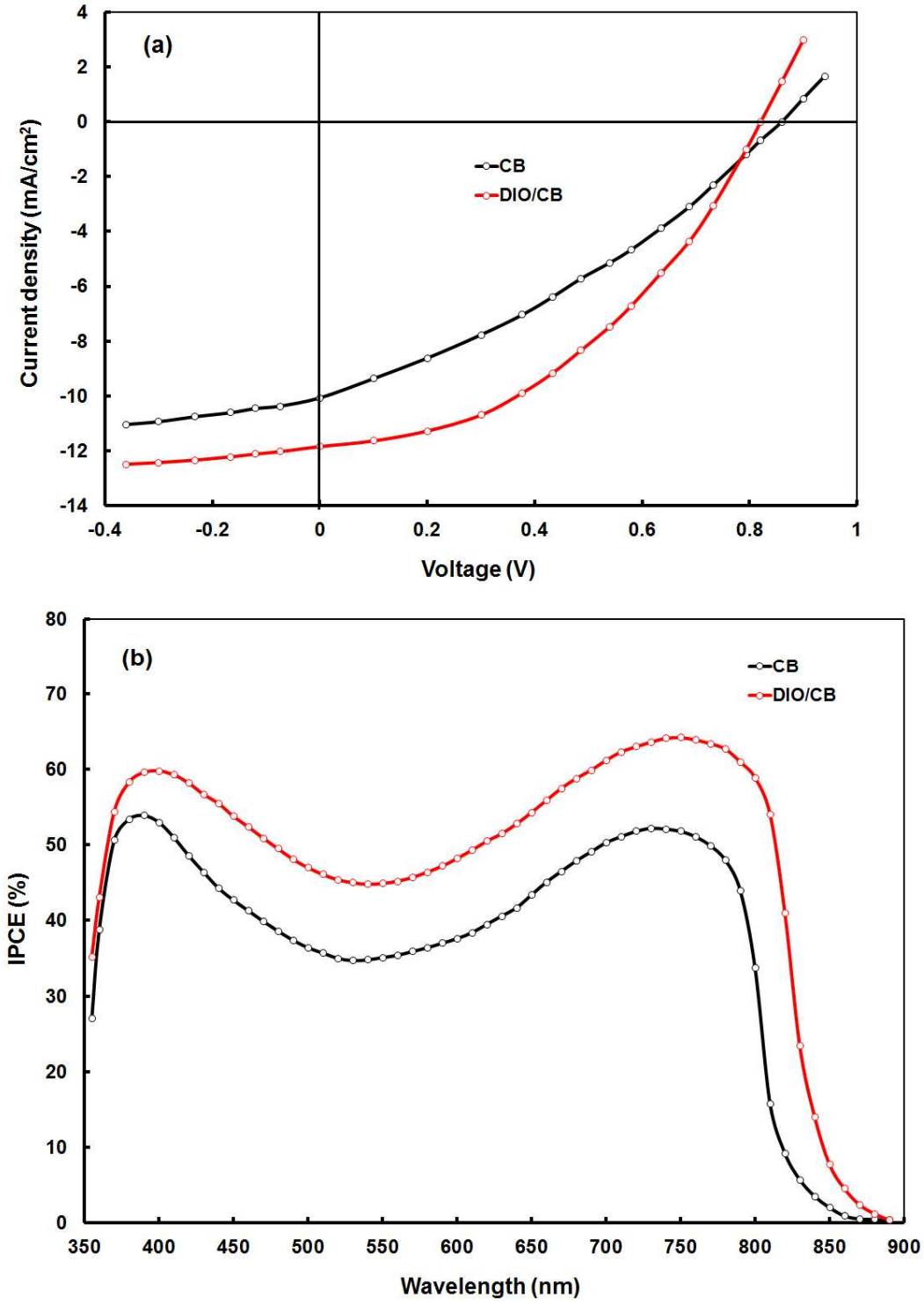

Figure 6(a) Current-voltage (J-V) characteristics and (b) IPCE spectra of **JK216D**:$PC_{71}BM$ BHJ organic solar cells, in which **JK216D**:$PC_{71}BM$ (1:2) spin cast with CB and DIO (3v%) /CB solvents.

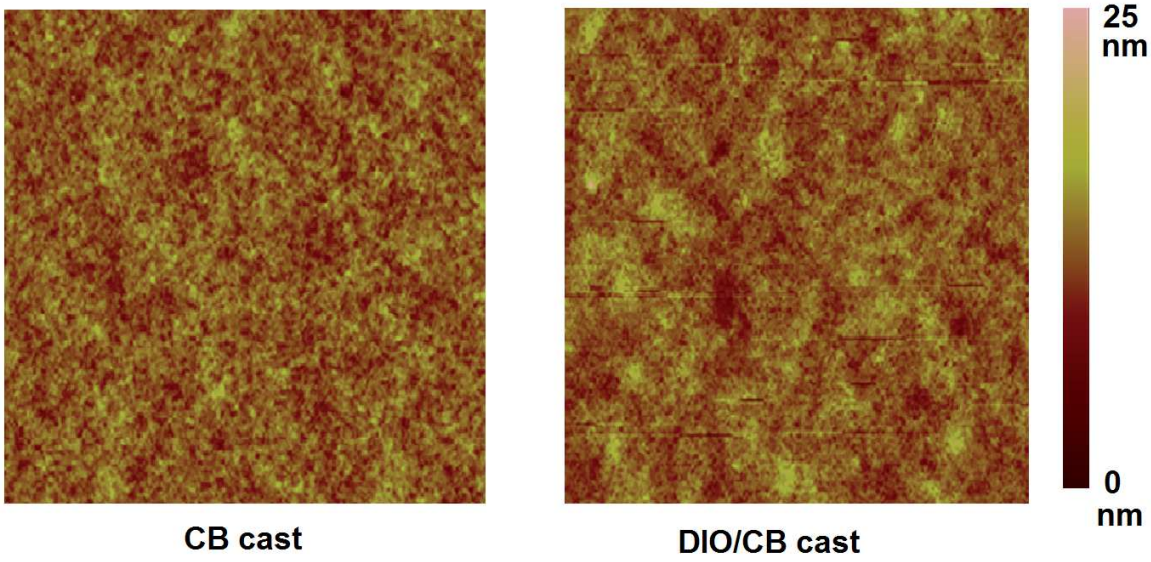

Figure 7 AFM images of **JK216D**:$PC_{71}BM$ films cast from CB and DIO/CB solvents. The image sizes are 3μm x 3μm.

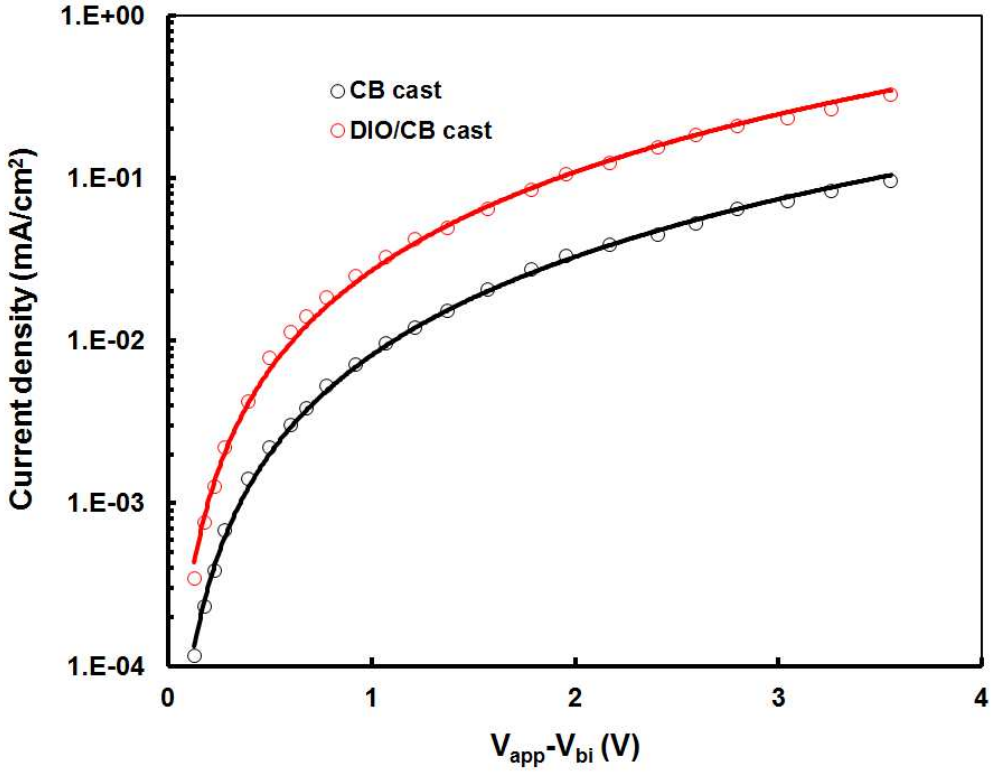

Figure 8 Current –voltage characteristics of hole only devices based on **JK216D**:$PC_{71}BM$ blends cast from CB and DIO/CB solvents. The solid lines are SCLC fitting.

TOC